

Recycled and Flexible Boron Nitride Heat Spread Film with High Thermal Conductivity

Jianxiang Zhang ^{a, b}, Xiangdong Kong ^{a, b}, Yandong Wang ^b, Zhenbang Zhang ^b, Linhong Li ^b, Kang Xu ^b, Maohua Li ^b, Rongjie Yang ^b, Yiwei Zhou ^b, Tao Cai ^b, Wen Dai ^b, Cheng-Te Lin ^{b, c}, Kazuhito Nishimura ^b, Zhongbin Pan ^{a, *}, Nan Jiang ^{b, c, *}, Jinhong Yu ^{b, c, *}

^a School of Materials Science and Chemical Engineering, Ningbo University, Ningbo, Zhejiang 315211, China.

^b Key Laboratory of Marine Materials and Related Technologies, Zhejiang Key Laboratory of Marine Materials and Protective Technologies, Ningbo Institute of Materials Technology and Engineering, Chinese Academy of Sciences, Ningbo 315201, China.

^c Center of Materials Science and Optoelectronics Engineering, University of Chinese Academy of Sciences, Beijing, 100049, China.

***Correspondence and requests for materials should be addressed to Z. Pan (Email: panzhongbin@163.com); N. Jiang (jiangnan@nimte.ac.cn) or J. Yu (Email: yujinhong@nimte.ac.cn)**

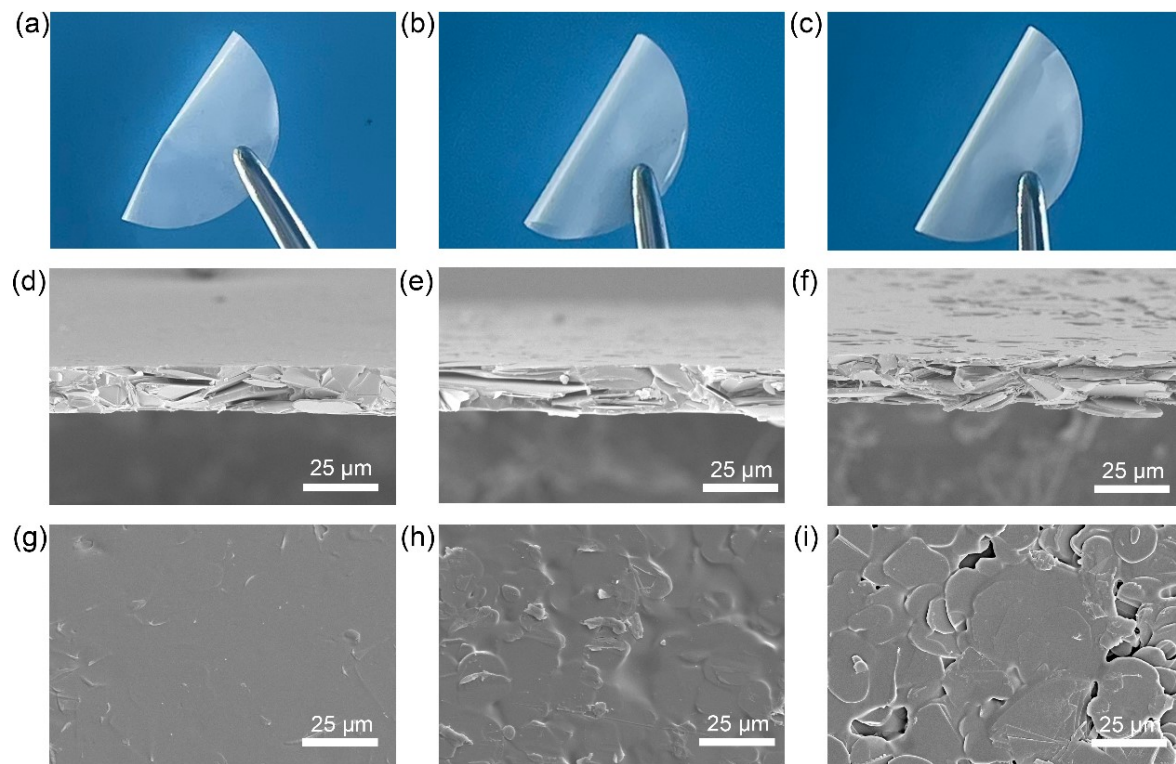


Figure.S1 (a-c) Digital photographs of 55,65 and 75wt% BNHS-VHP composite films. (d-f) Cross-sectional SEM images of 55,65 and 75wt% BNHS-VHP composite films. (g-i) Surface SEM images of 55,65 and 75wt% BNHS-VHP composite films.

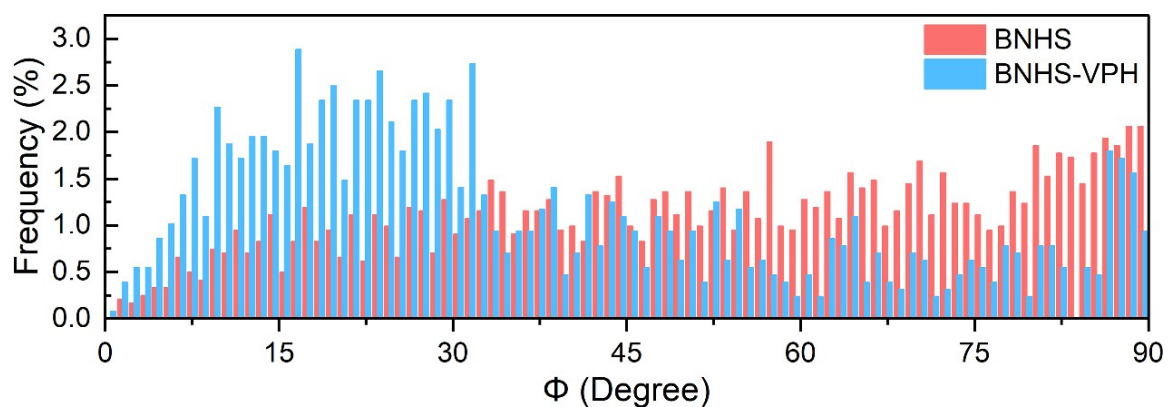


Figure.S2 Frequency distribution plot of the angle Φ between the direction of the normal vector to the h-BN and the through-plane direction, based on the micro-CT model.

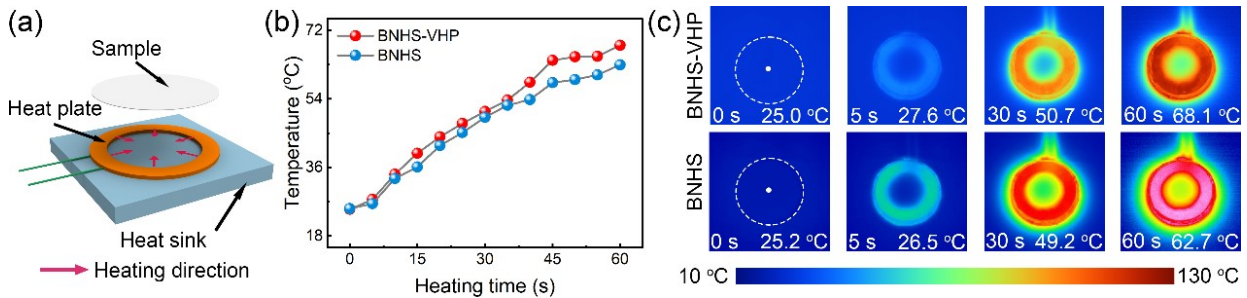


Figure.S3 (a) Schematic of the experimental setup. (b) The central temperature change of the BNHS and BNHS-VHP as a function of running time. (c) IR images corresponding to the BNHS and BNHS-VHP

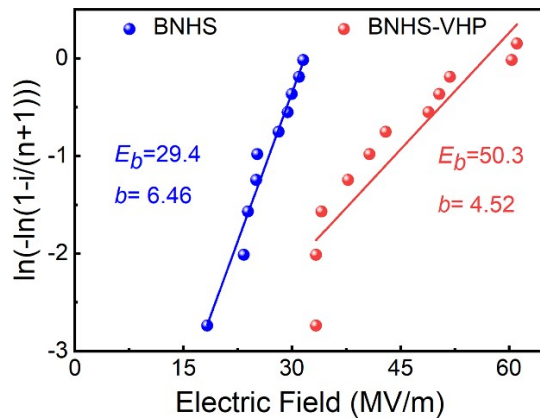


Figure.S4 Weibull plots and determined characteristic breakdown strength.

As a heat spread film for electronic devices, the electrical insulation performance of the composite material film is also of great concern. The values of E_b for BNHS and BNHS-VHP were obtained from a two-parameter Weibull statistical analysis. Fig. S5 presents the E_b and b values for BNHS and BNHS-VHP. It can be observed from the test results that the non-vacuum hot-pressed BNHS exhibits a lower E_b compared to BNHS-VHP. This can be attributed to the presence of surface defects and a higher number of voids in the non-vacuum hot-pressed BNHS. In contrast, the vacuum hot-pressing process applied to BNHS-VHP reduces the presence of voids, resulting in enhanced density and a decreased presence of defects. Therefore, the E_b value for BNHS-VHP is higher than that of BNHS. Furthermore, the b value for BNHS is larger, indicating a less uniform distribution compared to BNHS-VHP. This further demonstrates that the vacuum hot-pressed BNHS-VHP exhibits

improved dielectric performance.

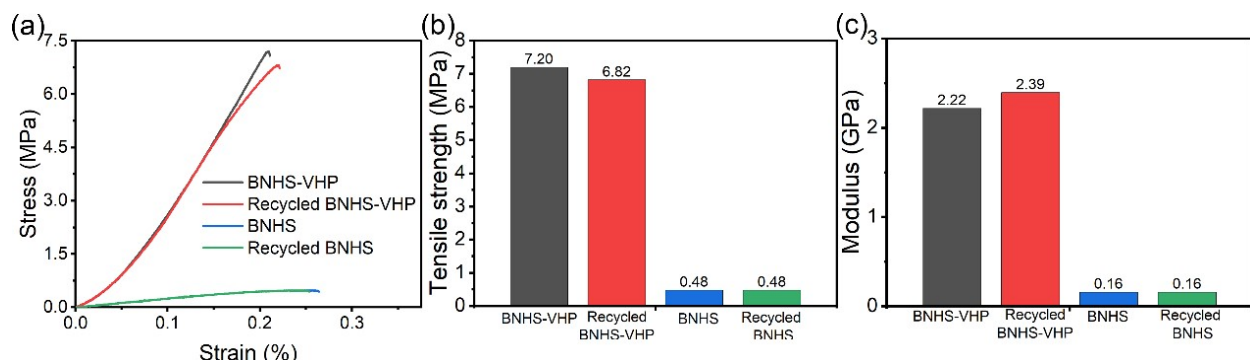


Figure S5 The mechanical properties of the composite films. (a) The stress–strain curves, (b) tensile strength, (c) Young's modulus of the different composite films.

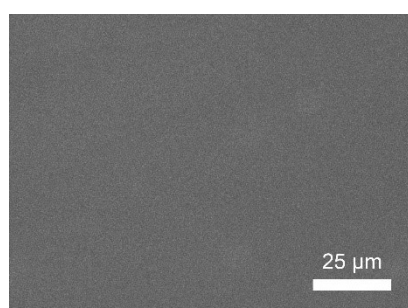


Figure. S6 Surface SEM images of pure PVB films.

Table S1. BNHS and BNHS-VHP heat spread films surface roughness.

	BNHS	BNHS-VHP
S _a	7.26 μm	2.32 μm
S _z	93.27 μm	54.80 μm
S _r	0.86	0.88
S _{pc}	712.69 1/mm	573.34 1/mm
S _{dr}	0.4512	0.1876

Table S2. The parameters for the calculation of in-plane thermal conductivities of BNHS and BNHS-VHP composite films at 25°C.

Sample	Thermal diffusivity (mm ² s ⁻¹)	Specific heat capacity (J g ⁻¹ K ⁻¹)	Density (g cm ⁻³)	Thermal conductivity (W m ⁻¹ K ⁻¹)
BNHS-VHP	44.691			73.459
	44.565	0.998	1.647	73.252
	44.674			73.431
BNHS	23.480			18.533
	23.441	0.983	0.803	18.503
	23.247			18.350

Table S3. The parameters for the calculation of through-plane thermal conductivities of BNHS-VHP and BNHS composite films at 25°C.

Sample	Thermal diffusivity (mm ² s ⁻¹)	Specific heat capacity (J g ⁻¹ K ⁻¹)	Density (g cm ⁻³)	Thermal conductivity (W m ⁻¹ K ⁻¹)
BNHS-VHP	0.150			0.247
	0.150	0.998	1.647	0.247
	0.149			0.245
BNHS	1.896			1.497
	1.878	0.983	0.803	1.482
	1.879			1.483

Table S4. A comparison of the In-plane thermal conductivity of composite films with different h-BN contents after vacuum hot-pressing at 25°C.

h-BN content (wt%)	Thermal diffusivity (mm ² s ⁻¹)	Specific heat capacity (J g ⁻¹ K ⁻¹)	Density (g cm ⁻³)	Thermal conductivity (W m ⁻¹ K ⁻¹)
55	19.794			22.228
	18.988	1.110	1.012	21.323
	18.698			21.516
65	24.559			30.497
	22.935	1.050	1.183	28.481
	22.650			28.127
75	37.237			47.413
	36.334	1.001	1.272	46.263
	36.229			46.129
85	44.691			73.459
	44.565	0.998	1.647	73.252
	44.674			73.431

Table S5. Comparison of thermal conductivity of composite films with different BN contents.

Samples	BN loading (wt%)	TC (W m ⁻¹ K ⁻¹)	Ref.
PVA/BNNS	22.2	21.4	S1
BNNS-OH/CNF	25	22.67	S2
ANF/BNNS	30	46.7	S3
ND/BNNS/PVA	30	15.49	S4
PVDF/BNNS	33	16.3	S5
ANF/BNNS@Ag	40	11.51	S6
BNNS/CNF	50	24.66	S7
BNNS/EVA	50	13.2	S8
CNF/OH-BNNS	50	15.13	S9
BNNS-GFS/CNF	67.5	55.65	S10
BNNS-Gly/CNF	70	16.2	S11
BN/PVB	85	73.38	This work

Reference

- (S1) J. Chen, H. Wei, H. Bao, P. Jiang and X. Huang, ACS Appl. Mater. Interfaces, 2019, 11, 31402–31410
- (S2) Z. Hu, S. Wang, G. Chen, Q. Zhang, K. Wu, J. Shi, L. Liang and M. Lu, Compos. Sci. Technol., 2018, 168, 287–295.
- (S3) K. Wu, J. Wang, D. Liu, C. Lei, D. Liu, W. Lei and Q. Fu, Adv. Mater., 2020, 32, 1906939.
- (S4) K. Zhao, G. Liu, W. Cao, Z. Su, J. Zhao, J. Han, B. Dai, K. Cao and J. Zhu, POLYMER, , DOI:10.1016/j.polymer.2020.122885.
- (S5) J. Chen, X. Huang, B. Sun and P. Jiang, ACS Nano, 2019, 13, 337–345.
- (S6) L.-H. Zhao, Y. Liao, L.-C. Jia, Z. Wang, X.-L. Huang, W.-J. Ning, Z.-X. Zhang and J.-W. Ren, Polymers, 2021, 13, 2028.
- (S7) L. Chen, C. Xiao, Y. Tang, X. Zhang, K. Zheng and X. Tian, Ceram. Int., 2019, 45, 12965–12974.
- (S8) Z.-G. Wang, W. Liu, Y.-H. Liu, Y. Ren, Y.-P. Li, L. Zhou, J.-Z. Xu, J. Lei and Z.-M. Li, Compos. PART B-Eng., , DOI:10.1016/j.compositesb.2019.107569.
- (S9) D. Hu, W. Ma, Z. Zhang, Y. Ding and L. Wu, ACS Appl. Mater. Interfaces, 2020, 12, 11115–11125.
- (S10) W. Qiu, W. Lin, Y. Tuersun, M. Ou and S. Chu, Adv. Mater. INTERFACES, , DOI:10.1002/admi.202002187.
- (S11) X. Tian, N. Wu, B. Zhang, Y. Wang, Z. Geng and Y. Li, Chem. Eng. J., 2021, 408, 127360.